Module 3: Velocity Measurement

Lecture 14: Analysis of PIV data

The Lecture Contains:

- Flow Visualization

- Test Cell Flow Quality

- Influence of End-Plates

- Introduction To Data Analysis

- Principle of Operation of PIV

  - Various Aspects of PIV Measurements
  - Recording of the Particle Images
  - Evaluation of Image Pairs
  - Peak Direction and Displacement Estimation
  - Data Validation
  - Dynamic Velocity and Spatial Range
  - Calibration Of PIV

◀ Previous   Next ▶

Flow Visualization

Many of the most exciting discoveries in the field of fluid mechanics have been possible due to careful flow visualization. Flow visualization allows us to gain an overall view of flow patterns. It helps in identifying the vortex structures and other secondary flow features. The introduction of tracer particles and the study of their movement provides considerable information of the flow physics. In liquids, colored dyes and gas bubbles are common tracers, whereas for gas flows, smoke, helium-lled `soap' bubbles or gas molecules made luminous by an ionizing electric spark have served as tracers.For the present investigation, flow visualization was carried out in the test cell using light generated from the pulsed Nd:YAG laser. Visualization was carried out in the nearwake region of the cylinder. The flow was seeded with small diameter oil droplets that were produced by the commercial particle generator discussed in Seeding Arrangement For PIV. There is an important difference between the nature of seeding for flow visualization compared to that of PIV measurements. In the latter, seeding is spatially homogeneous with a high particle density. The homogeneously seeded images appear featureless i.e. no flow structure is visible. Structures become visible only when the velocity field is evaluated. During flow visualization, seeding is done in an inhomogeneous manner. It clusters around the cylinder and the seeding density is reduced to highlight the flow structures. The CCD camera is once again synchronized with the ring of the laser, though image pairs are not required. The images of the CCD camera are each of 1280 $\times$ 1024 pixels. During experiments, images were acquired through a PC at a rate of 8 Hz. The light sheet and the camera were perpendicular to each other. The particle traces were further processed with an imaging software (Paint-shop available with MS-Windows) to improve clarity.
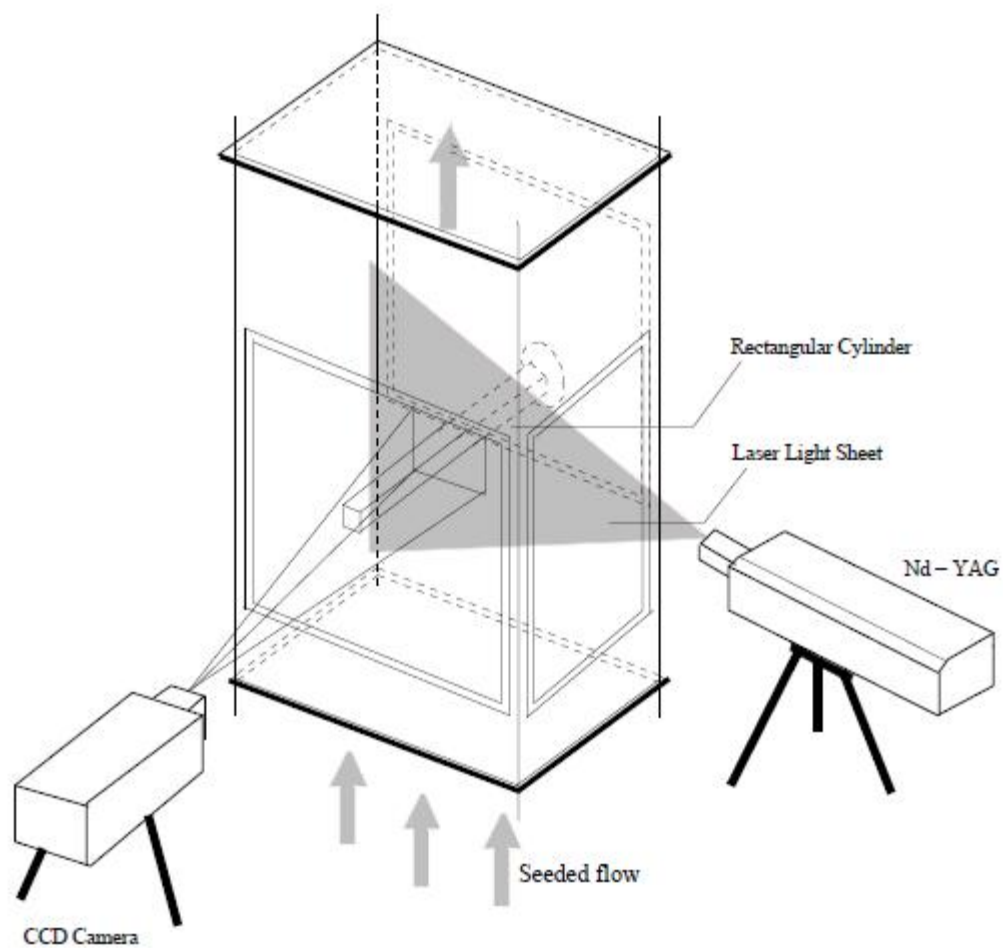
Figure 3.24: Schematic drawing of the flow visualization arrangement.

Rectangular Cylinder

Laser Light Sheet

Nd – YAG

Seeded flow

CCD Camera

◀|||Previous   Next|||▶

Test Cell Flow Quality

The inlet flow turbulence level and the flow parallelism have been tested for flow quality of the test cell. Figure 3.25 shows representative vector plots at two different velocity settings from PIV measurements. The turbulence level in the incoming flow is equal to 0.06% (Figure 3.26). The turbulence intensity was measured from the hotwire signal. The test cell flow parallelism has been presented in Figure 20. Flow parallelism in the approach flow is better than 98% over 95% of the width of the test cell. Uniform and stable free stream velocities in the range 0.5-3 m/s were realized in the test cell to cover the Reynolds number range of 100-800. Figure3.27 (a) also compares the velocity from pitot static tube with that from PIV. The excellent comparison between the two techniques indicates successful implementation of the optical imaging procedure.
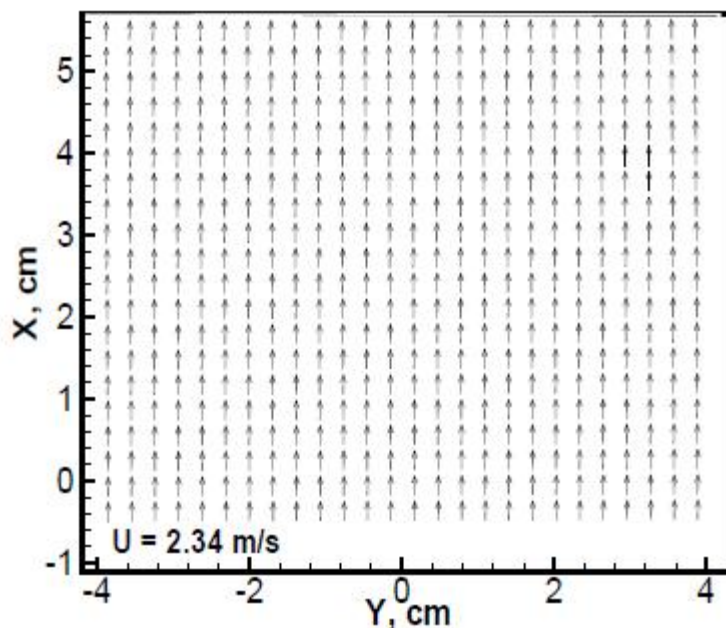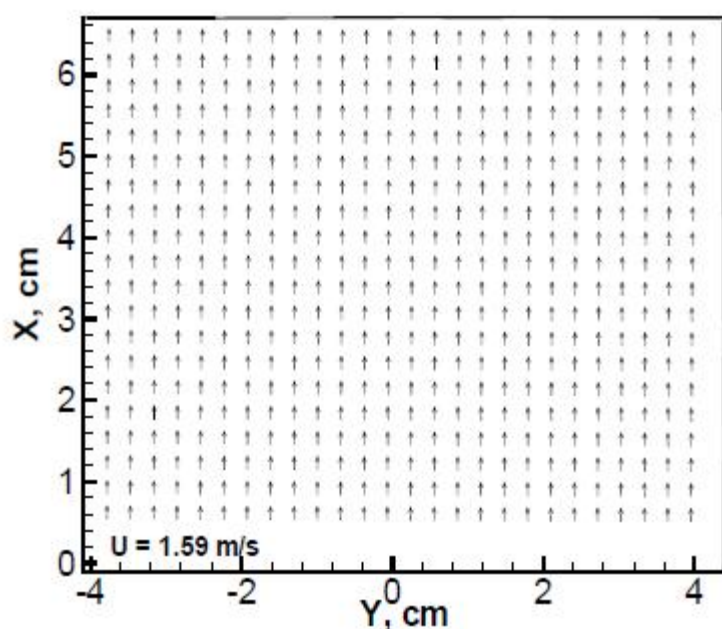
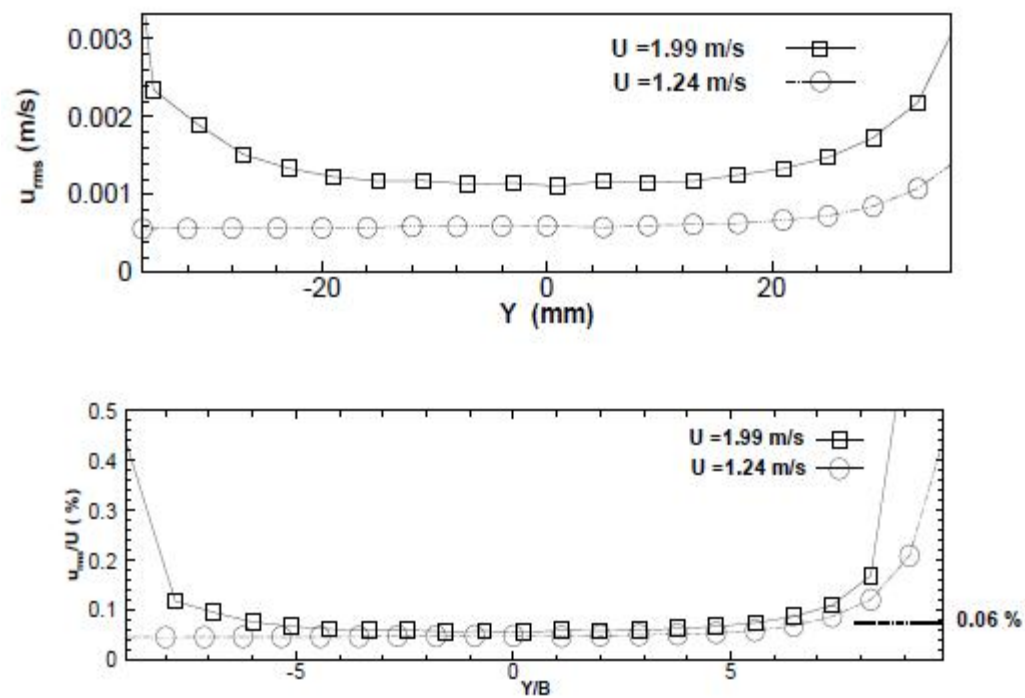**Figure 3.25: Time-averaged free stream velocity vectors from PIV at two blower settings**

Figure: 3.26 Turbulence level of the incoming ow measured by the hotwire anemometer. The average incoming velocity is denoted as U. The top and the bottom figures show dimensional and non-dimensional values respectively.

◀‖ Previous   Next ‖▶

Influence of end-plates

The effect of end conditions on the aerodynamics behind bluff bodies is a known fact. The wake stability and the critical Reynolds number are also influenced by the aspect ratio of the cylinder. End plates reduce three-dimensional effects, i.e. they shield the cylinder from the interfering wall boundary layers. Different designs of end plates have been proposed in the literature. The effect of aspect ratio on the wake structure is also affected by the end plate design. Measurements were done with and without endplates. Extensive iterations of the endplate geometry and their angle to the incoming flow were carried out to ensure parallel vortex shedding. The endplate parameters are based on work of Stansby (1974) and Norberg (1994). The base pressure can be reduced by suitably designing the end plates to keep the flow two dimensional (Stansby, 1974).
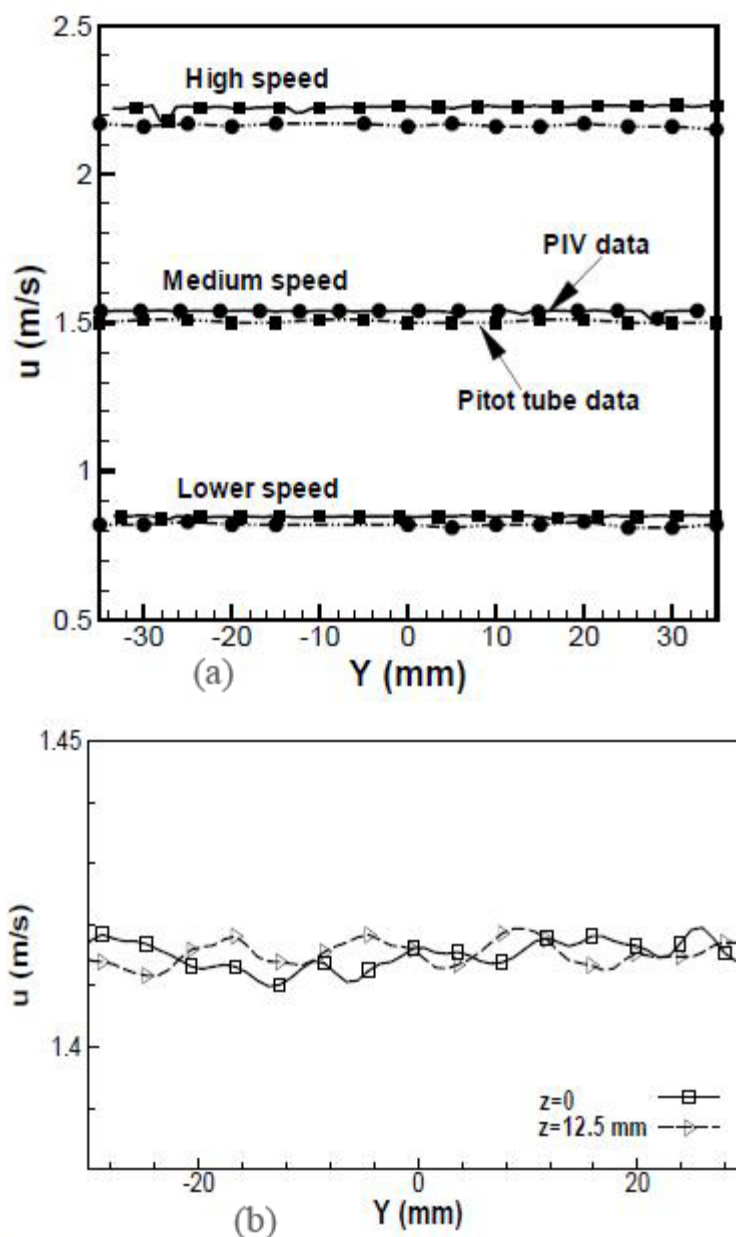
Figure 3.27: (a) Velocity profile of the incoming flow in the test cell from PIV and Pitot static tube measurements at three different tunnel speed settings (b) The incoming velocity prole at two dierent spanwise planes. The coordinate z = 0 falls on the vertical mid-plane of the test cell.

The distance of the cylinder axis from the outlet of the contraction is around ten times the cylinder edge to ensure adequate decay of free stream disturbances (Sohankar et al. (1998)). The velocity profiles behind a square cylinder with and without endplates are compared at the midplane and at an offset location (z = 5) for three downstream locations (x = 2; 5 and 10) (see Figures 3.27 and 3.28). Results from two Reynolds number (Re=220 and 370) have been shown. The difference in the velocity profiles at different spanwise locations was found to be minimal for both configurations with and without end plates (except at x=10 and Re=370). At x=10 location, the effect of end plates is unclear. The low turbulence level in the test section along with thin boundary layers probably lead to a small wall effect. Hence no endplate has been used in the subsequent experiments. In the present study, the effect of cylinder oscillation on wake structure has also been reported. The use of end plates would have increased the experimental complexity required for the end plate arrangements.
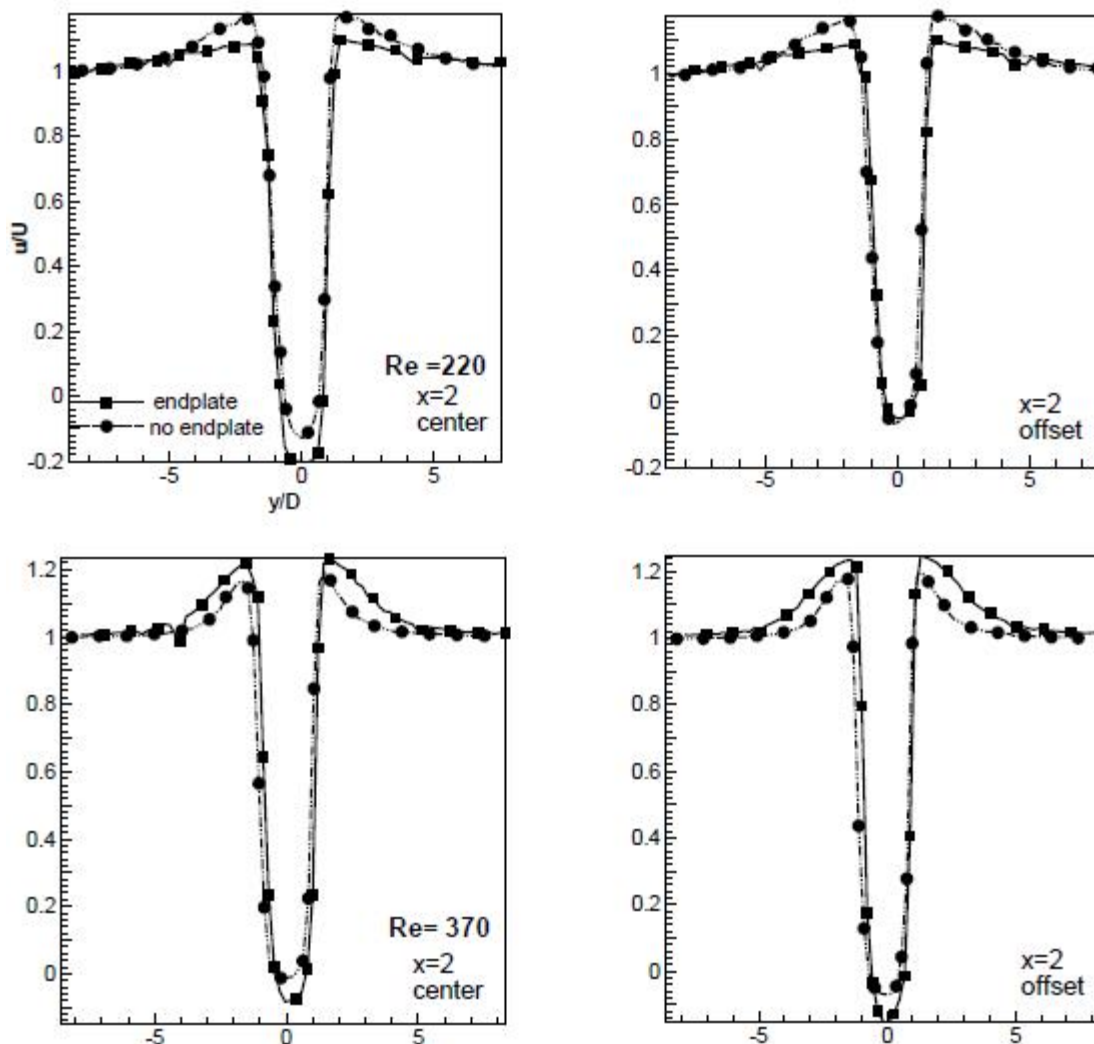

Figure 3.28: Effect of endplate on mean velocity profiles behind a square cylinder for two spanwise locations, z=0 (center) and z=5 (oset) at x=2. Reynolds number = 220 and 370.
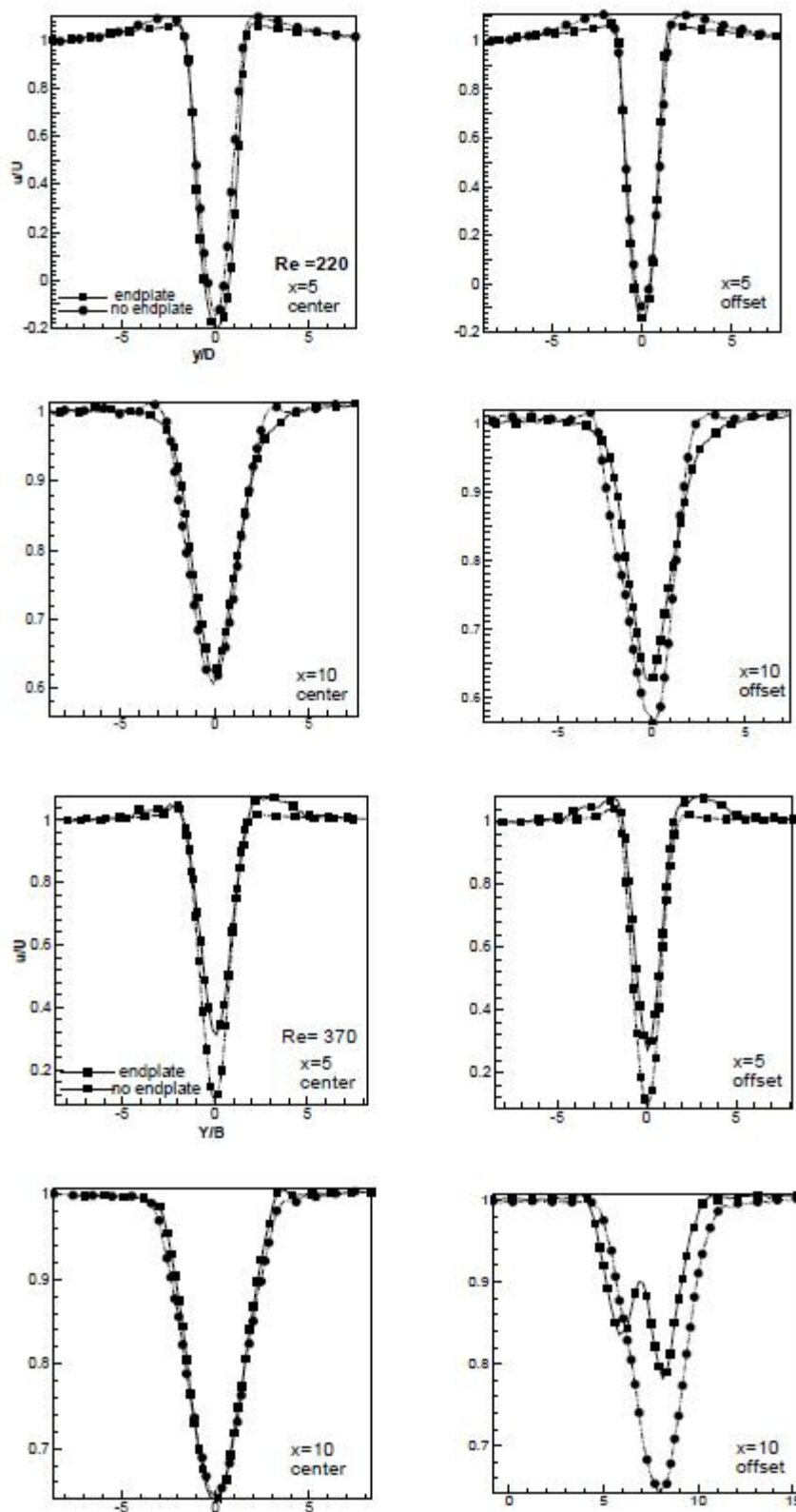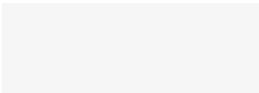
Figure 3.29: Effect of endplate on mean velocity profiles behind a square cylinder (Re=220 and 370). The result are shown at two dimensionless downstream locations (x=5 and 10) and two spanwise locations (z=0 and =5).

Objectives_template

Data Analysis

Introduction

In the present study, particle image velocimetry (PIV) and hotwire anemometry (HWA) have been used for velocity field measurements in the spatial and temporal domains respectively. These measurements have been used to calculate the mean and statistical quantities describing the flow, i.e. mean and rms velocities, power spectra, vorticity, drag coeffcient, Strouhal number and turbulent kinetic energy. The details of calibration and data analysis procedures for these quantities are discussed below. The proper implementation of the measurement techniques is validated by comparing the recorded data against each other. The uncertainty in measurements is reported from a repeatability study. The measurements, experimental procedure and data analysis are validated from a comparison of Strouhal number and drag coeffcient data with the published literature a comparison of Strouhal number and drag coecient data with the published literature.

Principle of Operation of PIV

Particle image velocimetry is a non intrusive technique for measuring the spatial distribution of the velocity within a single plane inside the flow The measurement is indirect, via the displacement of moving particle groups within a certain time interval. For this purpose the flow is seeded homogeneously with appropriate tracer particles. The concentration of the particles must be well adjusted with regard to the nest flow structures. It is assumed that the particles are small enough to move with the local flow velocity. A plane within the flow is illuminated twice within a short time interval by a laser sheet.

The duration of the illumination light pulse must be short enough that the motion of the particle is frozen during the pulse exposure in order to avoid blurring of the image. The light from each pulse scattered by the tracer particles is recorded by a CCD sensor on separate frames. The time delay between the illumination pulses must be long enough to be able to determine the displacement between the images of the tracer particles with suffcient resolution. It should be short enough to avoid particles with an out-of-plane velocity component leaving the light sheet between subsequent illuminations. Analyzing one image pair, it is possible to identify the path a particle has traveled. Knowing the time delay between the two pulses, velocity can be calculated. The time interval between two pulses has to adjusted according to the mean ow velocity and the magnication of the camera lens. The particle displacement Δx must be small relative to the nest flow scale to be resolved.

After finding the displacement of each interrogation spot, the quantity is divided by Δt and the magnification factor M of the image system to calculate the first order approximation of the velocity field as follows:

$$\int_t^{t+\Delta t} u(t')dt' \approx \Delta x$$

Hence

$$\frac{\Delta x}{\Delta t} = \frac{\Delta X}{M \Delta t} \approx u$$

Correlation-based PIV has the advantage over particle tracking algorithms in which each particle path is followed. In contrast, in correlation based PIV, the average motion of small group of particles contained in the interrogation spot is calculated by spatial auto correlation or cross correlation. Auto correlation is performed when images for both laser pulses are recorded on the same sensor, while in cross correlation, each pulse is collected into separate frames. Cross correlation calculation becomes faster in the frequency domain since the FFT algorithm is now applicable. There is directional ambiguity in auto correlation technique. Hence, in case of reversed flow, this technique is not suitable. The drawback can be eliminated using the cross correlation technique. Cross correlation allows us to use a small interrogation area compared to auto correlation and leads to a reduction of the random error due to spatial velocity gradients. An important condition involves depth of field of recording optics and laser light sheet thickness. Generally, depth of the field should not be smaller than the thickness of the light sheet in order to avoid imaging out-of-focus particle.
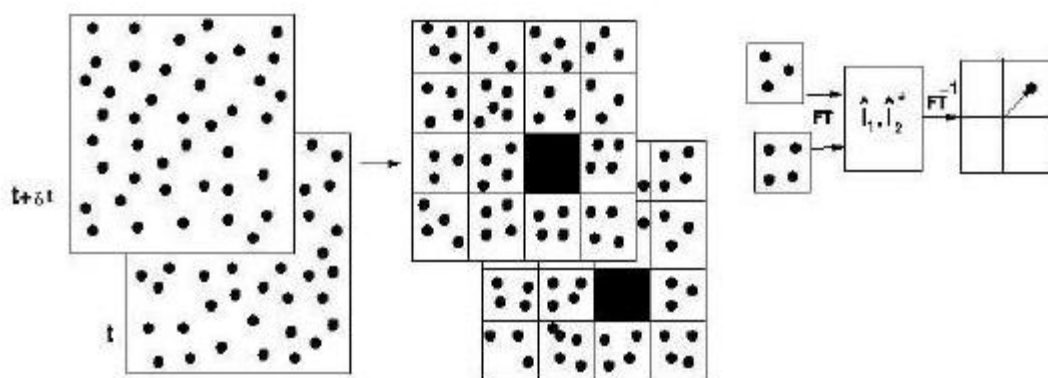

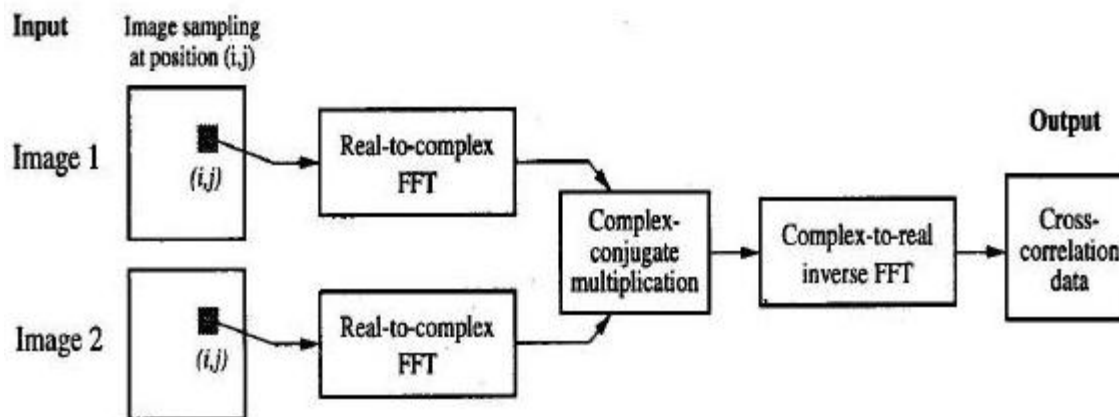**Figure 3.30: Cros Corellation analysis of a piv Image Pair**

Figure 3.31: Computation of cross correlation using FFT.

◀❙❙ Previous   Next ❙❙▶

Various aspects of PIV measurements

There are various aspects that should be taken into consideration while doing PIV measurements. Starting from image capturing to ultimately converting the image information into velocity vectors, each step requires proper validation. As already mentioned, the tracer particles should follow the flow faithfully without much velocity lag. Correspondingly, the tracer particles should be homogeneously distributed in the flow field. They should be small enough to follow the fluid movement and large enough to be visible.

A set of six non-dimensional parameters that are most signicant for optimization of PIV measurements were identified by Keane and Adrian (1990). These are the data validation criterion, the particle image density, the relative in-plane image displacement, the relative out-of-plane displacement, a velocity gradient parameter and the ratio of mean image diameter to the interrogation spot diameter. Two terms which are frequently used in PIV measurements are source density

$$N_s = \frac{C\Delta_{zo}}{M_o^2}\frac{\pi}{4}d_\tau^2$$

and the image density

$$N_I = \frac{C\Delta_{zo}}{M_o^2}D_I^2$$

Here, C is the tracer particle concentration $[m^{-3}]$, $\Delta_{zo,}[m]$ light sheet thickness M_o image magnification, d_τ particle image diameter [m] and D_i is the interrogation spot diameter [m]. The source density represents the type of image that is recorded. A source density larger than unity means that the image is a speckle pattern and when the source density is less than unity, the image consists of individual particle images. The image density represents the mean number of particle images in an interrogation region. It should larger than 10-15 for a good PIV measurement.

The optimal pulse separation between two images is influenced by a number of parameters. Two main types of error affect the choice of pulse separation (Δt) very much. These are random error and acceleration error. Random error arises from noise during recording of images and subsequent interrogation of the particle images. Acceleration error arises from approximation of Lagrangian motion of tracer particle to local Eulerian velocity based on small particle displacement. These two kinds of errors contradict the selection of pulse separation. The random error contribution can be reduced by increasing Δt but acceleration error increases as Δt increases. At some intermediate value of Δt, the total error should be a minimum. The optimum separation can be derived by considering these two errors as

$$\Delta t_{opt} = \sqrt{\frac{2cd_\tau}{M|dv/dt|}}$$

Previous   Next

In order to evaluate the correlation correctly with a single pass, the correlation function must be small with respect to the displacement correlation peak. This is accomplished when the following requirements are fulfilled:

1. There should be at least 7-10 particle image pairs in each interrogation spot.

2. The in-plane displacement should be limited to 1/4 of the size of the interrogation region.

3. The out-of-plane displacement should be limited to 1/4 of the thickness of the light sheet.

4. The displacement difference over the interrogation volume should be less than 3-5% of the size of the interrogation region.

Recording of the particle images

Besides particle dynamics, the registration, storage and read-out of the individual particle images are other key elements in PIV. This is because the accuracy of the technique is strongly depends upon the precision with which the image displacement can be related to particle locations and their respective particle displacements. The continuous intensity distribution of the particle image is transformed into a discrete signal of limited bandwidth. When the discretization of the image signal matches the minimum sampling rate, the frequency contents of the original signal, and thus the particle location as well, can be reconstructed without any losses. According to the well-known Nyquist criterion of signal processing, the bandwidth limited signal can be perfectly reconstructed from its discrete samples when the sampling rate of the signal is at least twice the signal bandwidth.

◀‖ Previous   Next ‖▶

Evaluation of image pairs

Statistical evaluation technique is used to extract information of the displacement from the two single exposed grey level patterns acquired at t and t'. Statistical evaluation technique is suitable since individual particle image pair detection is not possible for high resolution PIV measurement. It is less sensitive to noise and image discretization errors. In this technique, the whole image is sampled with an appropriate step size. For each sampling location, a two dimensional grey level sample $I\,(x, y)$ of certain shape and size is extracted from the source image. It is cross correlated with the corresponding sample $I'\,(x, y)$ from the second image.

In general, the cross-correlation function is given by

$$R(x, y) = \sum_{i=-k}^{k} \sum_{j=-l}^{l} I\,(i, j)I'(i + x, j + y)$$

Here I and I' are intensity values of the image pair. The cross correlation function produces a signal peak when the images align with each other, since the sum of the product of the pixel intensities will be larger than elsewhere.

In general, calculation of the correlation function is done in the Fourier space. For FFT analysis the data should be periodic. There are other issues such as aliasing and bias errors that need to be taken into consideration. Each subregion is transformed into the Fourier space via a Fourier transformation. The sub-windows are the spatially shifted and their Fourier transforms determined until the correlation is found. The correlation values are weighted accordingly to reduce bias error.

The cross correlation of two functions is equivalent to a complex conjugate multiplication of their Fourier transforms. In actual applications, the formulas used are

$$R \leftrightarrow \hat{I}\,\hat{I}'$$

where $\hat{I}$ and $\hat{I}'$ are the Fourier transforms of the image intensities I and I'.

◀|| Previous   Next ||▶

Once the correlation is found, the Fourier transformations are converted back into the physical space. The displacement that yields a maximum in the correlation function over the interrogation area is regarded as the particle displacement. Actually it is not the particle displacement which is computed but the displacement of the interrogation area. The displacement vector is of first order, i.e. the average shift of the particles is geometrically linear within the interrogation window. The size of the interrogation should be suffciently small such that the second order effect, i.e. displacement gradients can be neglected.

Peak detection and displacement estimation

One of the important steps in evaluation of PIV images is to measure the position of correlation peak accurately to sub-pixel accuracy. To increase the accuracy in determining the location of the displacement peak from ± 0.5 pixel to sub-pixel accuracy, an analytical function is fitted to the highest correlation peak by using the adjacent correlation values. Various methods of estimating the location of the correlation peak have been proposed. Some of these are peak centroid fit, Gaussian peak fit and the parabolic peak fit. Of the three, the Gaussian fit is most frequently used to estimate the shape of the signal around its peak assuming ideal imaging conditions. This function is

$$f(x) = C_o \exp - [-\frac{(x_o - x)^2}{k}]$$

where x_o indicates the exact location of the maximum peak and C_o and k are parametric coeffcients. Using this expression for the main and the adjacent correlation values and the fact that the first derivative of this expression at x_o must be zero, the position can be estimated with sub-pixel accuracy. Generally, a 3-point Gaussian peak fit gives good results. When the particle image size is small, the displacement tends to bias towards integer values. The assumed peak shape does not match the actual shape of the peak and the three point Gaussian estimator cannot represent the true shape of the correlation function. This is called the *peak-locking effect*. In actual displacement data, the presence of the peak-locking effect can be detected from histogram plot.

Data validation

In particle image velocimetry the measurements contain a number of spurious vectors. These vectors deviate unphysically in magnitude and direction from the nearby vectors that are, in turn, physically meaningful. They originate from those interrogation spots that contains insuffcient number of particle images, or whose signal to noise ratio is very low. In post processing process, the first step is to identify these bad vectors and subsequently discard them to form a valid data set. The detection of either a valid or spurious displacement depends on the number and spatial distribution of particle image pairs inside the interrogation spot. In practice, there should be at least four particle image pairs to obtain an unambiguous measurement of the displacement (Westerweel, 2000). The number of particle images inside an interrogation spot is a stochastic variable with a Poisson probability distribution. Hence an average of 10 particle images per interrogation spot at an average in-plane displacement of $\frac{1}{4}D_I$ will give a probability of 95% of finding at least four particle image pairs. Here, D_I is the size of the interrogation spot. The valid data yield can be improved by increasing the seeding density. But by increasing the seeding density we increase the influence of the seeding on the flow.

There are various way to detect spurious vector in a velocity field. Three mainly used tests are the global mean test, local mean test and local-median test. The global mean and the local mean are both linear estimators of valid vectors. The local median test is a nonlinear estimator that is often used in outliers identification. The outliers in turn, are identified by the median of the sample data. Out of the above three, Westerweel [176] has shown that the local median test has the highest effciency. In these techniques, the value at a grid point is compared with the neighboring grid points; if it exceeds a certain threshold, the value is discarded.

◀‖ Previous   Next ‖▶

For the present analysis, multi-pass interrogation technique has been applied. In the first evaluation, the images were sub-divided into 64×64 pixel non-overlapping interrogation images. The corresponding sub-images in the translated image and the reference image were analyzed by computation of the cross-correlation function. Since there was no overlap between adjacent interrogation images, each pair yielded 320 statistically independent displacement vectors. In the second evaluation, a 32×32 pixel interrogation window was used with an overlap of 50%. The corresponding resolution is 0.5 mm and 5120 vectors were recovered from one pair of images. All measured integer displacements that deviated more than one pixel from the expected displacement were considered as spurious vectors. They were subsequently discarded from the data set. Such a strict test for spurious data can only be done if one has a priori knowledge of the displacement field.

Dynamic velocity and spatial range

Dynamic spatial range is related to spatial resolution and dynamic velocity range is related to the fundamental velocity resolution and hence, the accuracy of a PIV. Dynamic velocity range (DVR) specifies the range of velocity over which measurements can be made. It is the ratio of the maximum velocity to the minimum resolvable velocity, or equivalently the RMS error in the velocity measurement, i.e.

$$\text{DVR} = \frac{U_{max}}{\sigma_u} = \frac{U_{max}}{\sigma_{\Delta x} M_o^{-1} \Delta t^{-1}}$$

where M_0 is the image magnification and Δt is the maximum time interval used for the experiments. The RMS error of the displacement field on the pixel plane ($= \sigma_{\Delta x}$) generally lies between 1-10% and so

$$\sigma_{\Delta x} = 0.1 (d_e^2 + d_r^2)^2$$

where d_r represents the resolution of the recording medium that is taken to be equivalent to the pixel size, and d_e is the diameter of the particle image prior to being recorded on the pixel plane. Assuming that the particle image is diffraction limited and its image intensity is Gaussian, the diameter of the diffracted image of the particle is expressed as:

$$d_e^2 = M_o^2 d_p^2 + [2.44(1 + M_o)f^\# \lambda]^2$$

◀‖ Previous   Next ‖▶

Here d_p is the seeding particle diameter, $f^\#$ is the F-number of the imaging lens and λ is the laser wavelength. For the present experiments, image magnification is $M_o = 0.04$, the pulse interval $\Delta t = 70\ \mu s, d_r$ represent the pixel size $(= 6.7\ \mu m)$, $f^\# = 1.4$, particle diameter $d_p \approx 2\ \mu m$ yielding a dynamic velocity range of 30. The dynamic spatial range (DSR) is defined as the ratio of the maximum resolvable scale to the minimum resolvable scale, i.e.

$$\text{DSR} = \frac{L_x/M_o}{U_{max}\,\Delta t}$$

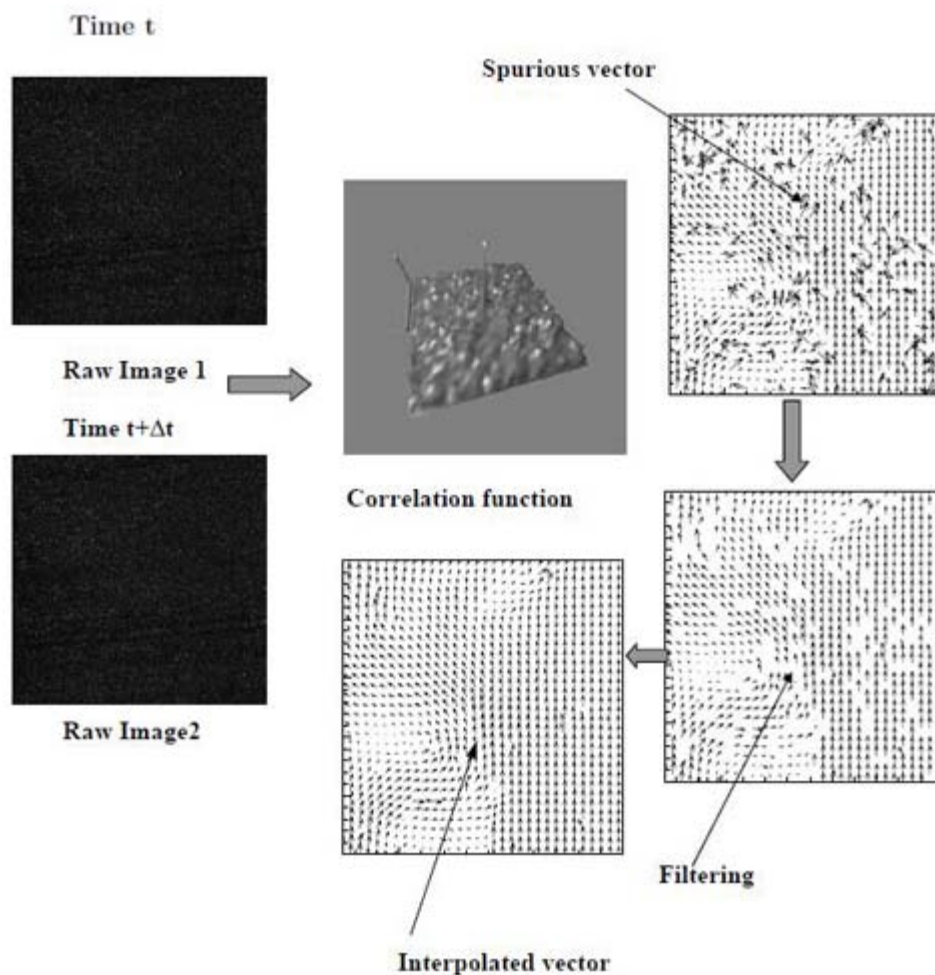where the CCD pixel array dimension $L_x = 8.85$ mm and DSR $= 1020$.

Figure 3.32: Processing of PIV images

Previous   Next

Calibration of PIV

To convert the velocity field from image coordinates to laboratory coordinates, length calibration is performed with a calibration sheet. Calibration sheet is a set of grid points on which the distance between two grid points is 10 mm. By putting the calibration sheet at the image plane, the image of the grid is captured and superimposed on the PIV image. Two types of calibration are followed depending upon the geometry of the flow field: linear and nonlinear calibration. In the case of plane geometry with a distortion free image, linear mapping is adequate. In this route, a minimum of four grid points is required. At the four grid points x and y coordinates of the image are specified and the corresponding pixel numbers identified from the image. By linear interpolation, all other x and y-coordinates are calculated for each pixel location. Once we get the real coordinates of each pixel of the image, the velocity vectors can be determined from the time interval between two images. Nonlinear calibration is recommended when image distortion is expected during recording by the camera.

Previous   Next